Radiation Physics and Chemistry 78 (2009) 859–873

Contents lists available at ScienceDirect

Radiation Physics and Chemistry

journal homepage: www.elsevier.com/locate/radphyschem

Geometry and physics of the Geant4 toolkit for high and medium energy applications ☆

J. Apostolakis [a], M. Asai [l], A.G. Bogdanov [j], H. Burkhardt [a], G. Cosmo [a], S. Elles [f], G. Folger [a], V.M. Grichine [a,g], P. Gumplinger [m], A. Heikkinen [e], I. Hrivnacova [d], V.N. Ivanchenko [a,b,*], J. Jacquemier [f], T. Koi [l], R.P. Kokoulin [j], M. Kossov [a,c], H. Kurashige [i], I. McLaren [a], O. Link [a], M. Maire [f], W. Pokorski [a], T. Sasaki [h], N. Starkov [g], L. Urban [k], D.H. Wright [l]

[a] CERN, Geneva, Switzerland
[b] EMSU, Moscow, Russia
[c] ITEP, Moscow, Russia
[d] IPN Orsay, France
[e] Helsinki Institute of Physics, Helsinki, Finland
[f] LAPP, Annecy, France
[g] Lebedev Physical Institute, Moscow, Russia
[h] KEK, Tsukuba Ibaraki, Japan
[i] Kobe University, Kobe, Japan
[j] MEPhI, Moscow, Russia
[k] RMKI, Budapest, Hungary
[l] SLAC, Stanford, USA
[m] TRIUMF, Vancouver, Canada

ARTICLE INFO

PACS:
07.05.Tp
13
21.60.Ka
23
02.70.Uu

Keywords:
Simulation
Monte Carlo
Particle interactions
Geometrical modeling
Nuclear interactions
Electromagnetic interactions
Hadronic interactions

ABSTRACT

The current status of the Geant4 toolkit and the recent developments for the geometry, electromagnetic and hadronic physics for medium and high energy are presented. The focus of many recent improvements of the toolkit are key applications including the simulation of large Hadron collider (LHC) experiments at CERN. These developments and physics model extensions provide new capabilities and improvements for other applications of the toolkit for radiation studies in high energy physics (HEP), space and medical research.

1. Introduction

Geant4 is a toolkit for Monte Carlo simulation of the transportation and interaction of particles in matter (Geant4 Collaboration, 2003; Allison et al., 2006). Its design is based on an object-oriented technique and it is implemented in C++. The development and the maintenance of the toolkit are provided by the international Geant4 Collaboration. Geant4 has been used for detector simulation since 2002 when it was adopted for use by the BaBar experiment at SLAC (BABAR Collaboration, 2002). The total number of events produced for BaBar is above 10^9 (Smith, 2004) and is rapidly increasing. Now Geant4 has become an established tool, used in the Monte Carlo production for three large hadron collider (LHC) experiments since early 2004 (Stavrianakou, 2004; Rimoldi, 2004; Mato et al., 2004). It is applied in many other high energy physics (HEP) experiments and in medical, space and other research (Allison et al., 2006; Amako et al., 2005; Jan et al., 2004; Santin et al., 2005).

☆ Thanks to organizers of the Workshop on Use of Monte Carlo Techniques for Design and Analysis of Radiation Detectors, 15–17 September, Coimbra, Portugal. This work was supported in part by the European Organization for Nuclear Research (CERN); by the Stanford Linear Accelerator Center (SLAC) through a grant from the US Department of Energy; by the Helsinki Institute of Physics.

* Corresponding author at: CERN, Geneva, Switzerland.
E-mail address: Vladimir.Ivantchenko@cern.ch (V.N. Ivanchenko).

0969-806X/$ - see front matter © 2009 Elsevier Ltd. All rights reserved.
doi:10.1016/j.radphyschem.2009.04.026

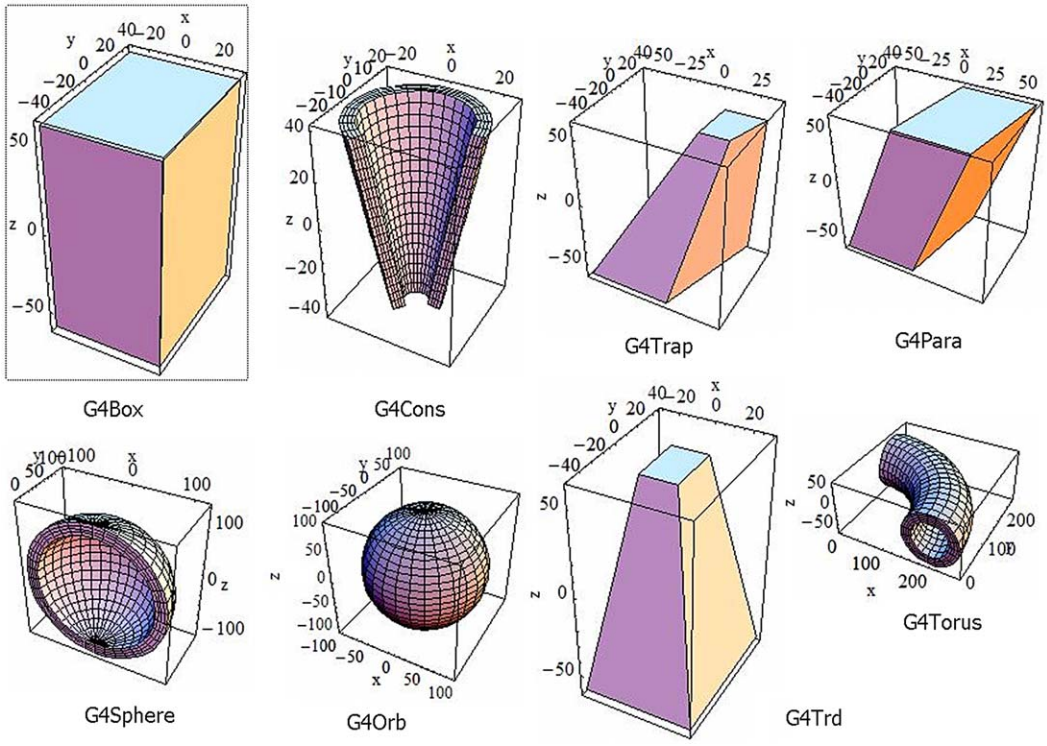

Fig. 1. Basic CSG shapes.

Geant4 includes components for geometry description, particle definition, navigation and tracking, physics models for electromagnetic (EM), hadronic and optical interactions, event scoring, input/output and visualization. The infrastructure for selectively applying fast shower parameterizations instead of simulation of detailed physics processes is also provided. Configurations of physics models tailored for large scale simulations, for single detectors, for dosimetry and for other applications have been recently developed and are now part of the toolkit. The progress in physics performance is monitored with validation efforts and physics comparisons against data both inside the Geant4 teams and in collaboration with different experiments and user groups.

The complete description of the toolkit is available on the Geant4 WWW pages (http://cern.ch/geant4). In this work key elements of the recent progress in a number of components of the toolkit are presented, namely in the geometry, materials, standard electromagnetic physics and hadronic physics. The developments in these domains have a direct impact on Geant4 applications for radiation detectors at high and medium energies.

2. Detector description

2.1. Geometry shapes

The geometry modeler (Geant4 Collaboration, 2003) is a key component of the Geant4 toolkit. It has been designed to allow the description of the geometrical structure of simple and complex detectors in a natural way, ranging from one up to hundreds of thousands of volumes of the LHC experiments. Human phantoms for medical applications, spacecrafts and planets for simulations in the space environment can also be modeled.

Geant4 provides the definitions of a wide variety of geometrical shapes (solids). Solids with simple shapes, like rectilinear boxes, trapezoids, spherical and cylindrical sections or shells, are available directly as constructed objects, according to the constructed solid geometry (CSG) specifications (Fig. 1). Functionalities provided by each of these solids have been recently reviewed to improve the accuracy in the response especially concerning the computation of normals on surfaces, edges and corners (Anninos et al., 2006). New geometrical shapes increased the rich set of primitives (Fig. 2), providing similar shapes with twisted (curved) sides.

Other solids (Boolean solids) can be obtained by combining constructed shapes with Boolean operations, like unions, intersections and subtractions. With Boolean solids one can describe complex particular shapes in a simple and natural way using well tested and efficient CSG solids. A new ability enables the computation of the geometrical volume and surface of any solid. For complex compositions or complex shapes, the value is estimated using a simple Monte Carlo technique tuned to obtain a typical accuracy at the level of 0.1%. Utilizing this, another ability is provided to compute the mass of a given setup.

2.2. Complex geometry

A detector setup's geometry is described by listing the different elements it contains and specifying their positions and orientations. A physical volume represents the spatial positioning of the volumes describing the detector elements, as positioned with respect to an enclosing (mother) volume. Structures of the detector that are repeated exactly can usually be described as one volume placed several times in different places. This can allow for great memory saving in case of complex structures. Volumes can be replicated or divided according to a regular structure or can be parameterized according to a user-specified formula applied to their shape, attributes and positioning. Only one instance of the physical volume will be finally created in memory. It is also possible to define nested parameterized

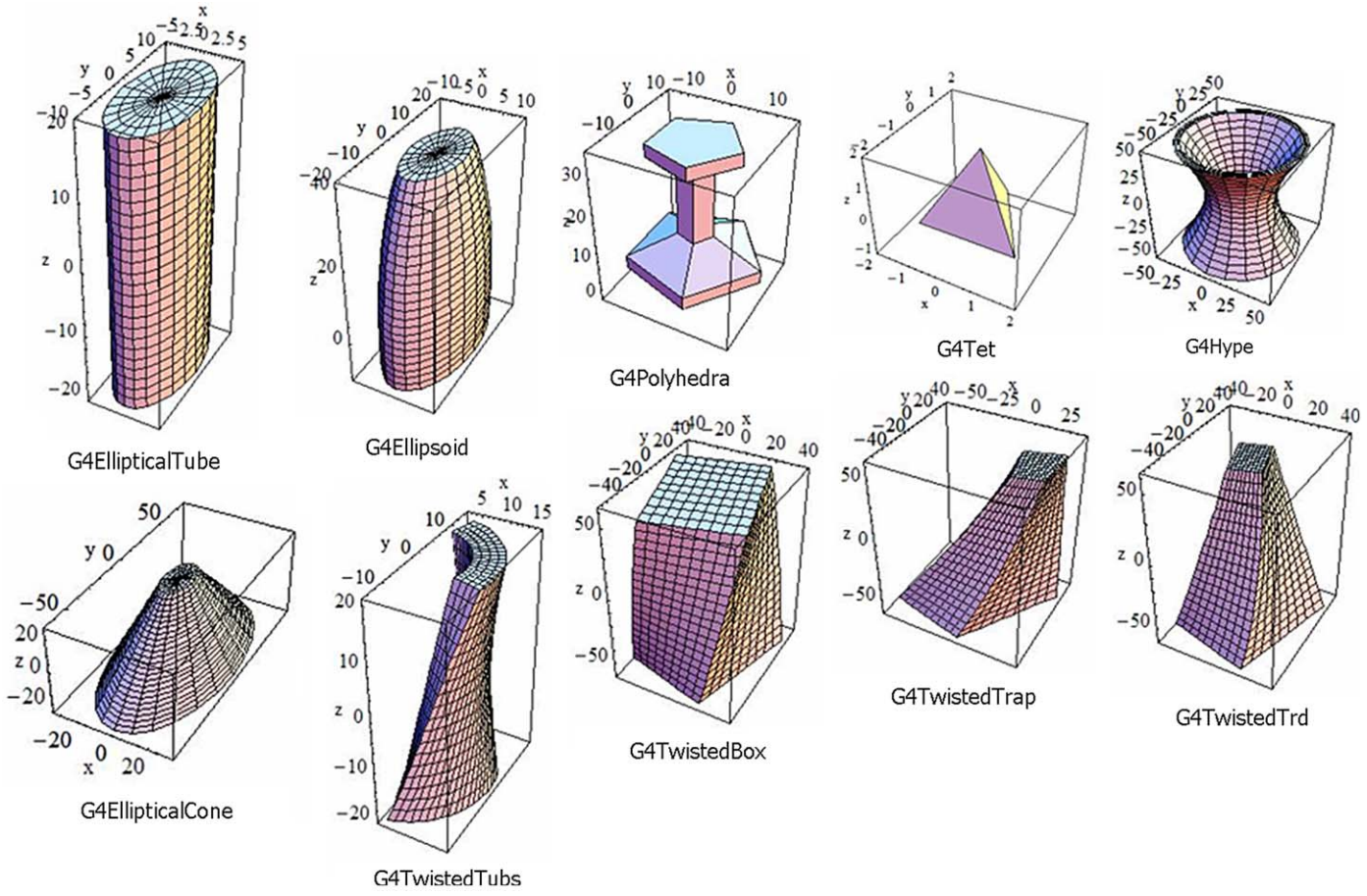

Fig. 2. New CSG shapes.

volumes, in which information from higher levels can be used to determine a volume material. This feature is particularly useful in the definition of voxelixed regular structures for usage in medical physics applications. The possibilities to group volumes as assemblies, or to automatically apply reflection to complete structures are available and integrated together with the rich variety of placement techniques already existing in Geant4.

A powerful technique recently introduced offers the option to determine overlaps at the time of creation of a geometrical setup. Activating a check when placing a single volume in the setup reveals if it overlaps with previously placed volumes. The placement of the volume is checked against the already existing volumes placed in the structure, by means of the generation of random points on the surface of the geometrical element being placed and verifying that none of the points are inside any other placed volume or outside of the mother volume. The adopted optimization technique greatly reduces the CPU time spent in computing volume intersections.

Importing and exporting persistent descriptions of the geometry is now possible thanks to the enhancements introduced in the GDML (geometry description mark-up language) schema, where now most of the shapes and positioning techniques of Geant4 are supported. GDML (Chytracek et al., 2006) makes possible geometry interchange between different applications, to allow for example, comparisons of different Monte Carlo engines, using the best features provided by their transportation algorithms and physics. It also allows to import/export geometry descriptions for usage in different visualization systems, since GDML defines an application independent format.

2.3. Internal database of materials

An internal Geant4 database of isotopes, elements and materials has been created. The goal of this development was to provide a simple method to describe media. The user can now create a new G4Material or G4Element using only the name in the database. By default an element is created with its natural isotope composition. Most of the data is obtained from the NIST databases (Coursey et al., 2005): natural isotope compositions, isotope masses, mean ionization potentials for elements and materials, material densities and atomic composition of materials. Some extra materials frequently used in simulation were also added to the database. Currently about 3500 isotopes, 108 elements, and about 300 materials are included. By default the natural isotope composition is created if an element is constructed from this database. The access to elements and materials is provided via its names, also the recent GDML software is capable of working with materials and elements built by this method. So, the usage of the Geant4 internal database on elements and materials benefits, because the user software becomes simpler and the data quality is guaranteed.

2.4. Other developments

The established advanced techniques for optimizing tracking in the geometrical model have been recently enhanced and are currently under evolution to address additional use-cases (Anninos et al., 2006). Special optimization techniques are

adopted and implemented in order to achieve efficient navigation during tracking and the best tuning of the navigation structure according to the geometrical topology of the model under consideration. The modeler has been recently extended by introducing the concept of a region (Allison et al., 2006) to 'tag' areas of a detector. Regions can be assigned to volume hierarchies (logical volumes) in Geant4 and can be associated to specific production cuts or cuts in range bound to particles.

The Geant4 geometry modeler also provides the way to apply event-biasing techniques, which can be associated to the geometrical description of a detector (Dressel, 2003). These are particularly useful for saving computing time in applications like for example the simulation of radiation shielding. The biasing techniques implemented so far are: geometrical splitting and Russian roulette (also called geometrical importance sampling), and weight roulette (Booth, 1985). Weights can be assigned to volumes in either the tracking geometry, or to volumes defining a parallel geometry imposed on the real one, and also where scoring techniques can be applied.

3. Standard electromagnetic physics

3.1. Geant4 electromagnetic sub-packages

Electromagnetic interactions of photons and charged particles with matter are implemented in two electromagnetic packages (Geant4 Collaboration, 2003). The 'Standard' EM package (Lassila-Perini and Urban, 1995; Apostolakis et al., 2000; Grichine, 2002; Urban, 2002) includes simulation of ionization, bremsstrahlung, gamma conversion and other EM interactions of particles with energies from 1 keV up to 10 PeV. Initially created to perform high quality Monte Carlo production for HEP experiments, it is now well applicable to space, medicine and other domains (Ivanchenko, 2002, 2004).

The 'Low-energy' EM package of Geant4 includes alternative models for simulation of photon, electron, hadron and ion interactions (Giani et al., 1999a, b; Apostolakis et al., 1999; Amako et al., 2005; Pia, 2003; Chauvie et al., 2004). It also includes models for simulation of atomic relaxation and other atomic shell effects, and unique models describing interactions of radiation with biological systems (Chauvie et al., 2006). The package is capable to describe interactions down to 100 eV and can perform very detailed simulation of particle transport in a media but requires significantly more CPU resources. Developments in the Low-energy package and its applications for radiation detectors are out of the scope of this paper.

The sub-packages for simulation of optical emission and transport (Geant4 Collaboration, 2003; Archambault et al., 2003) are also a part of the Standard EM package. Thus, a complete simulation can be performed starting from the beam transport all the way to the final radiation detector using electromagnetic packages. The detailed description of physics models and implementations is available in the Geant4 Physics Reference Manual (see details in Geant4 WEB). About 50 different examples of various applications of EM physics are provided together with the Geant4 toolkit.

The Standard EM package has been used for large scale productions since the beginning of the Geant4 distribution (Smith, 2004). At the same time, developments are continuing and improvements are introduced (Allison et al., 2006; Burkhardt et al., 2005; Bogdanov et al., 2006; Urban, 2006). To provide stability of the simulation results for long-term productions, in particular, for LHC experiments, a verification suite has been created (Apostolakis et al., 2006) and is executed on a regular base before each new Geant4 release. The most important recent developments are discussed below.

The design of the package (Burkhardt et al., 2005; Apostolakis et al., 2006) provides a clear separation of management functions from physics models by providing generic abstract classes. This design enables extensions of current models and creation of alternative implementations for the same physics process. User access to cross sections and stopping powers is provided via the *G4EmCalculator* class. It is possible to access these Geant4 values stored in tables, which are built at the initialization stage of Geant4. Also it is possible to compute cross sections and stopping powers on-fly for materials, which are not necessary a part of the detector setup. In the latter case, the elements and materials from the internal Geant4 database can be used.

3.2. Energy loss

Energy loss processes in Geant4 have continuous and discrete components (Geant4 Collaboration, 2003). High energy transfers of energy are simulated as real discrete acts of an interaction in which secondary δ-electrons and bremsstrahlung photons are generated. Low energy transfers are treated as a continuous process of energy loss. The mean value of this restricted energy loss is obtained as a result of the integration

$$\frac{dE}{dx} = -\int_0^{\varepsilon_{lim}} \varepsilon\sigma(E,\varepsilon)\,d\varepsilon, \tag{1}$$

where $\varepsilon_{lim} = \min(T_{cut}, T_{max})$, T_{cut} is the production threshold for the kinetic energy of secondary particles (δ-electrons or gammas) in the given material and T_{max} is the kinematical limit of the energy transfer. Thus, energy transfers below ε_{lim} are considered as continuous energy loss. For electrons and positrons the same integration is applied to the processes of ionization and bremsstrahlung. The sum of these two contributions is calculated at the initialization stage of Geant4 and stored in the form of the dE/dx table. Consecutively to that the range and the inverse range tables are also calculated. For testing purposes and for foreseen developments in Geant4 the additional dE/dx and range tables are calculated using infinite cut value. This allows accessing the total mean energy loss and the CSDA range of a particle at run time. Additionally the restricted cross section of each process is calculated and stored in the separate lambda tables:

$$\lambda(E) = -\int_{\varepsilon_{lim}}^{E} \sigma(E,\varepsilon)\,d\varepsilon, \tag{2}$$

where $\lambda(E)$ is the inverse interaction length. At each simulation step the restricted cross (2) is sampled using an integral approach and the restricted mean energy loss (1) is calculated. Taking into account this mean energy loss, the length of the step and material properties the fluctuation of the energy loss is sampled using the Geant4 model (Lassila-Perini and Urban, 1995). In order to have enough simulation steps the stepping function is used to limit the step size:

$$s = \max(\rho, \alpha R(E) + \rho(1-\alpha)(2-\rho/R(E))), \tag{3}$$

where s is the step limit, $R(E)$ is the current range, α is the step size range parameter and ρ is the minimal step size. The default value of $\alpha = 0.2$ is proven by many years of simulation practice. The default value $\rho = 1$ mm was chosen to be equal to the default Geant4 cut in range value. These defaults provide reasonable simulation results for transport of electrons and hadrons in uniform media, and are applicable to standard HEP applications. In a specific application, the user can tune these parameters of the stepping function. Note, that (3) is only the additional step limitation in Geant4, because the step limits are established also by other physics processes (Geant4 Collaboration, 2003).

Initially Geant4 implementation of the ICRU parameterization (Allisy et al., 1993) of the Bragg peak of ionization was provided in the Low-energy EM package (Giani et al., 1999a, b) and different validation studies have been performed (Amako et al., 2005; Cirrone et al., 2005), which show that both Geant4 EM packages describe well ionization of hadrons and ions. However, some problems were observed, in particular, non-precise parameterization of the proton stopping power in some materials up to 10% in the energy interval 1–5 MeV. To address these problems a number of improvements based on the review (Allisy et al., 1993) were provided for the simulation of ionization for hadrons and ions in the Standard EM package:

- new shell correction parameterization;
- Barkas correction;
- Bloch correction;
- Mott correction and
- nuclear stopping power.

These corrections are relatively small for hadrons and are more significant for ions. With the new parameterization the difference between proton stopping powers for different materials provided by the Standard EM package and the evaluated data (Allisy et al., 1993) is well inside 2% (Apostolakis et al., 2006), which is less than systematic uncertainty of the data. This development was triggered by the requirement to improve simulation of hadrons in LHC detectors but is also very important for simulation of hadron therapy and other applications.

3.3. Multiple scattering

The most important recent development has been introduced in the treatment of multiple scattering. The Geant4 model (Urban, 2002) was based on Lewis's (1950) approach. Originally both large and small simulation steps were allowed, with steps being limited by the ionization's limitation (3), by interaction length in a media and by geometry boundary. The model provides results, which are in good agreement with the data for high energy hadrons and electrons (Urban, 2002; Burkhardt et al., 2005). However, a number of reports noted on the strong dependence of results for sampling calorimeters on production cuts. Moreover, the analysis (Poon and Verhaegen, 2005) of energy deposition in a 1 MeV photon beam inside a low density cavity demonstrated that Geant4 results obtained with the default parameters vary from theoretical expectations (Fig. 3) and in order to obtain a precision on a percent level it is necessary to decrease artificially the step size.

To address this problem a refinement of the multiple scattering process and model was undertaken (Urban, 2006). It was mainly the concern of low energy electron scattering near geometry boundaries. Modifications were introduced in multiple scattering from Geant4 release 8.0:

- a correlation between scattering angle and lateral displacement (Kawrakow and Bielajew, 1998);
- the recalculation at each simulation step of the minimal distance to the geometric boundary;
- more strict step limitation near a boundary and
- an extra limitation of the step size for geometrical volumes, at least two steps inside a volume in which a particle starts and at least three steps inside other volumes.

These improvements provide more precise and stable results, at the cost of additional CPU cycles. The dependence of the energy

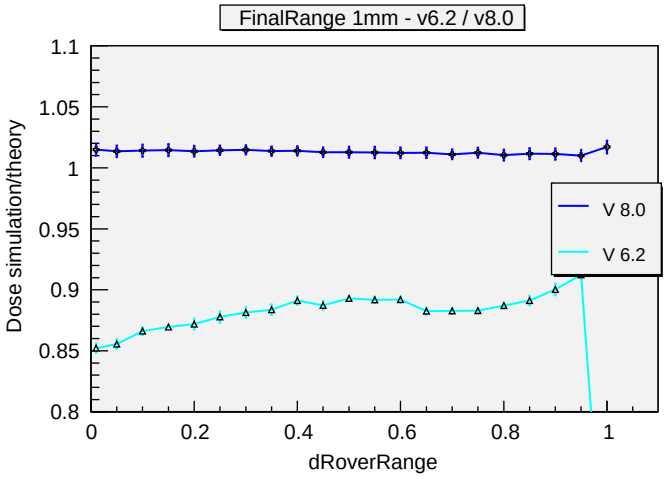

Fig. 3. The ratio of simulated and theoretically computed dose deposition inside water cavity filled with vapor water as a function of the stepping parameter α; the parameter $\rho = 1$ mm (default). Both parameters are used by Geant4 tracking for particle step limitation (see text). Points and solid line-G4 8.0p01, triangles and dashed line-G4 6.2p02.

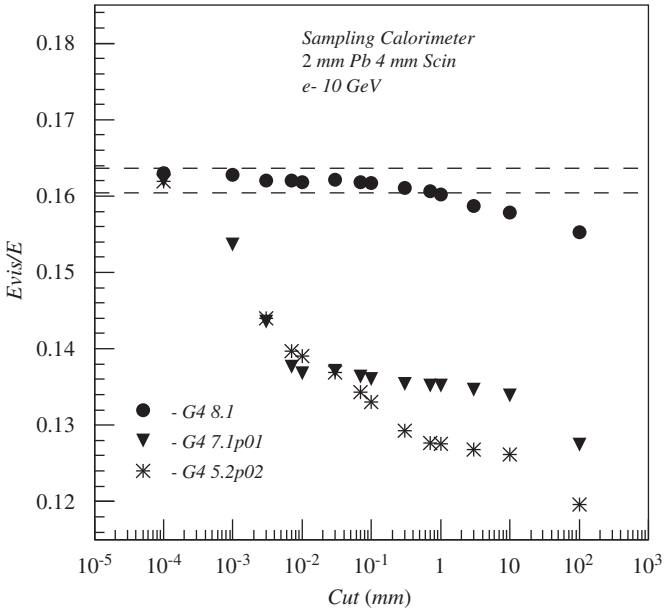

Fig. 4. Visible energy deposition in sampling calorimeter as a function of the production threshold (cut) for different Geant4 releases: dashed lines show ±1% variation around the limit value. The revised multiple scattering model of Geant4 8.0 shows significantly larger stability.

deposition inside a cavity as a function of the parameter α becomes stable and correct within 1% (Fig. 3).

Practical importance of the multiple scattering is illustrated by the simulation results for a lead/scintillator structure similar to the LHCb calorimeter. The increased stability is evident with 1% accuracy up to the cut value 0.3 mm (Fig. 4). Incident particles are electrons of 10 GeV, production cuts for electron and gamma are expressed in terms of the range cut (Geant4 Collaboration, 2003). These results are in agreement with those of Fig. 3, because the simulation of transport of secondary electrons from the high-density media (lead) to low-density media (scintillator) has been improved. The energy resolution of the calorimeter is also sensitive to the multiple scattering model (Fig. 5) and the new model demonstrate better stability of the results.

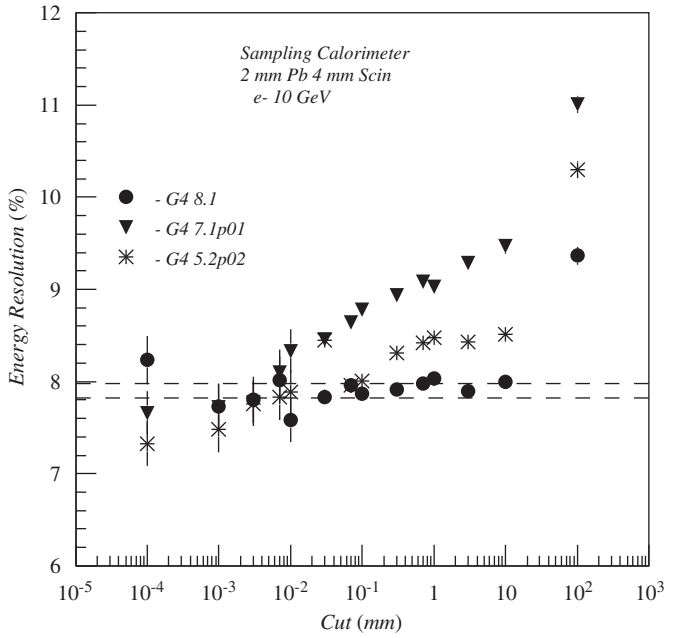

Fig. 5. Energy resolution of sampling calorimeter as a function of the production threshold for different Geant4 releases. Dashed lines show ±1% variation around the limit value.

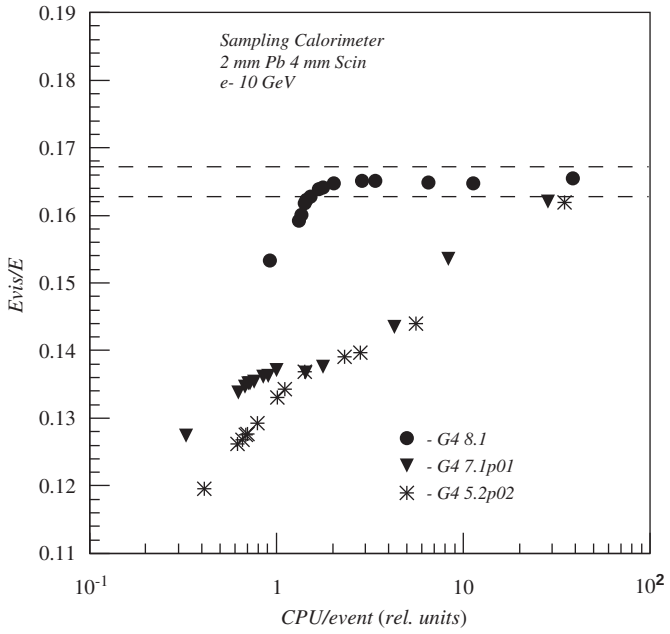

Fig. 6. Visible energy deposition in sampling calorimeter versus CPU time instead of cut (see Fig. 3) for different Geant4 releases. Dashed lines show ±1% variation around limit value. The best quality for much less CPU can be achieved with the revised multiple scattering model of Geant4 8.0.

The CPU performance of the simulation has a significant implication for the number of events that the LHC experiments can simulate. If the same cut value is used, then with the new multiple scattering model more time is required per event, which depending on cut and geometry, varies from 10% to 100%. However, in order to achieve the same accuracy of simulation results with the new model it is possible to use higher values of cuts, which is demonstrated in Fig. 6 where energy deposition is shown as a function of required CPU instead of cut. In this particular calorimeter, 1% precision is achieved with the Geant4 version 7.1 using the cut value 0.0001 mm and with version 8.1 using the cut 0.3 mm, respectively, so the required CPU time with version 8.1 and optimal cut is 20 times less.

3.4. Electromagnetic physics versus geometry

Initially in Geant4 a unique production threshold (*cut in range*) was used (Geant4 Collaboration, 2003). However, HEP detector simulation requires very high precision tracking of particles inside vertex detectors and high CPU performance for calorimeters and muon identifiers. In the Geant4 release 5.1 a design iteration across the toolkit has been done in order to provide the possibility to have different cuts for different sub-detectors or other geometrical regions (Allison et al., 2006). The production thresholds for photons, electrons and positrons are unique for each region. The mechanism of initialization and steering of the energy loss, range, and cross section tables was revised. At the beginning of the Geant4 run each vector of a table is recalculated, or retrieved from an external file, or left unchanged. The activation of retrieving is provided by a user command, the recalculation triggered if the material or any cut is changed. Several physics models for a given particle type can be applied depending on the particle energy. For example, for muon ionization there are three different models applicable for low, medium and high energies (Bogdanov et al., 2006) and all these models are working in the same simulation run.

The conception of regions can be used also to specialize the choice of physics model to a particular part of a setup. A standard EM process can use several underlying physics models. Before generation of secondary particles the process selects a model to apply depending on the energy of the projectile and now using the region. For example, the PAI model of ionization (Apostolakis et al., 2000) allows each secondary electron to be generated, relevant for the detailed simulation of gaseous detectors. This simulation is time consuming, so choosing to use the PAI model only for gas of ionization chambers (or for thin semiconductor layers) and not for the whole geometry of the detector provides significant performance benefits. This approach (Burkhardt et al., 2005) is an option in the GRAS tool (Santin et al., 2005), created for space radiation effect studies.

3.5. Integral approach

One of the important improvements of the package is the introduction of the integral approach in the mechanism of sampling of an interaction length. In the old design derived from Geant3 the interaction length for a given process was defined by the cross section in the beginning of the step (Geant4 Collaboration, 2003). In the revised algorithm the energy dependence of the electromagnetic cross sections for charged particles takes into account sampling of the interaction probability

$$p = 1 - \exp\left(-\int \sigma(E) n \, dx\right), \tag{4}$$

where $\sigma(E)$ is the cross section for the given energy, n is the atomic density and x is the coordinate along the trajectory. The sampling is performed using the method proposed in Ivanchenko et al. (1991). Before a step of a particle in the media for each process the maximum of the cross section over the step σ_{max} is estimated in the energy interval $\zeta E_0 - E_0$, where $\zeta = 1 - \alpha$ is the parameter (default value 0.8), E_0 is the particle energy at the beginning of the step. If this process is randomly chosen to limit the step, then the

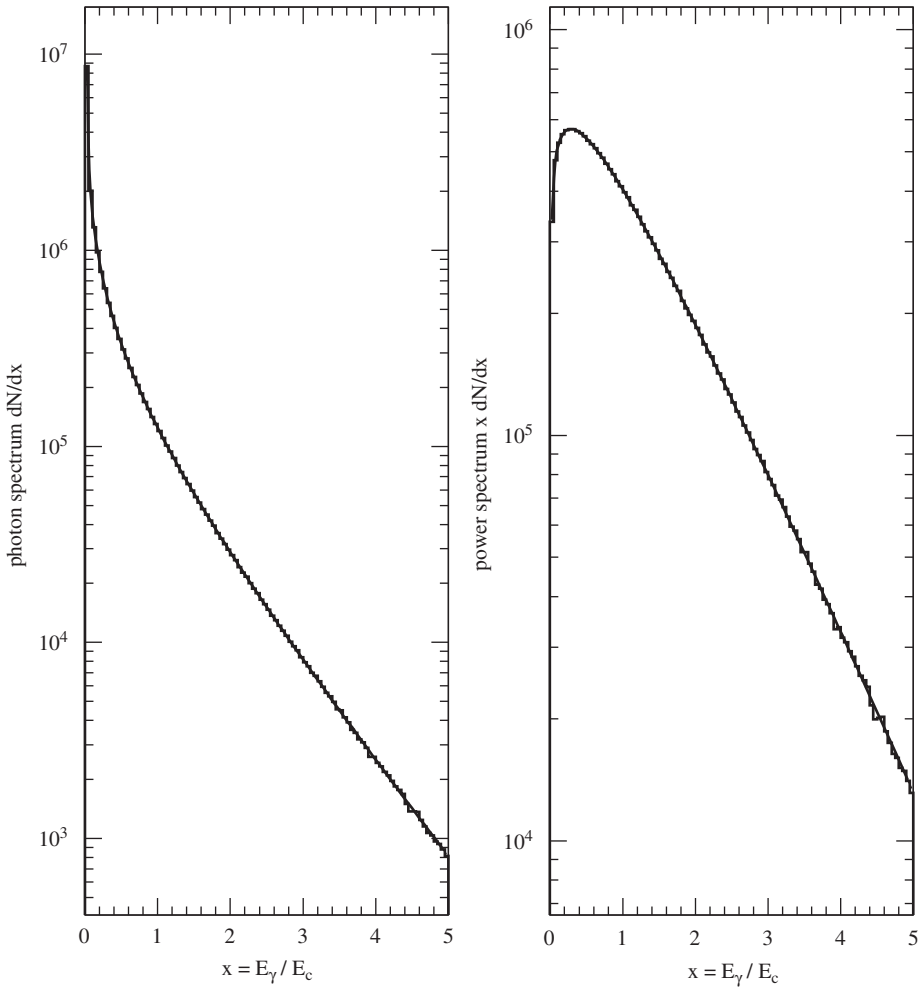

Fig. 7. Comparison of the theoretical (smooth curve) and generated (histogram) spectra of synchrotron radiation. The photon spectrum is shown on the left and the power spectrum on the right side. The simulation is practically coincide with the theory.

corresponding final state of the process should be sampled. After the step of the particle, its energy E_1 is different, so the changed value of the cross section $\sigma(E_1)$ is calculated and the sampling of the final state is performed not in all cases but randomly with a probability

$$p_S = \sigma(E_1)/\sigma_{max}, \tag{5}$$

that in fact is equivalent to the Monte Carlo integration of the cross section required in the relation (4). The method is absolutely precise and independent of the step size if the maximum value of the cross section is correctly estimated. Because of CPU performance reasons it is not practical to do a general determination of this value at each step. As the first estimation the value $\sigma_{max} = \max(\sigma(E_0), \sigma(\zeta E_0))$ is used, which is valid if the cross section continuously increases or decreases. Secondly, the check is performed when the absolute cross section maximum is inside the energy interval $\zeta E_0 - E_0$ using the peak position of the cross section which is determined during the initialization. If the check is positive the peak value is taken as σ_{max}. This approach is valid for all known EM cross section shapes.

3.6. Other developments

Modifications were recently introduced to the processes of transition radiation and synchrotron radiation. The transition radiation will be used for very high energy particle identification in LHC experiments. The synchrotron radiation process can be used at LHC; however, the main application area is electron beam transport in a magnetic field. A new, fast and very precise generator algorithm has been implemented. It is based on direct inversion of the cumulative distribution, using a small set of intervals, simple transformations and Chebyshev polynomials (Burkhardt, 2007). It is valid for the standard conditions: approximately homogeneous field and vacuum. The simulated spectra of photons coincide with the theoretical predictions (Fig. 7).

4. Hadronic physics

4.1. Hadronic models overview

In Geant4 applications in high energy and nuclear physics, hadronic interactions are handled by different models which cover the high, medium and low energy domains. The current standard set of models for HEP includes the quark–gluon string (QGS) (Folger and Wellisch, 2003), the Bertini-style cascade (Heikkinen et al., 2003), the Binary cascade (Folger et al., 2004), and chiral invariant phase space (CHIPS) (Degtyarenko, 2000, 2001a, b). These models are detailed and theory-based (as opposed to pure parameterization) and explicitly conserve

energy-momentum and most quantum numbers. The above models handle inelastic interactions of protons, neutrons, pions, kaons, hyperons. Other models (Geant4 Collaboration, 2003) are used to fill in the gaps in coverage and extend the capabilities of the package:

- the high precision neutron model for energies from thermal to 20 MeV;
- several elastic scattering models optimized for various energy ranges and
- several types of nuclear de-excitation codes, including fission, Fermi breakup and multi-fragmentation, which are used by other models.

There are also the low energy parameterized (LEP) and high energy parameterized (HEP) models which have their origins in the GHEISHA hadronic package (Fesefeld, 1985) which was used with Geant3. The GHEISHA Fortran code was cast into C++, re-engineered and split into the current high- and low-energy parts. Like the GHEISHA code, these models are intended to be fast, cover all long-lived particles and to describe hadronic showers reasonably well. They are also intended to conserve energy and momentum on average but not event by event.

4.2. Quark–gluon string model

The QGS model (Folger and Wellisch, 2003) is used in Geant4 to simulate the interaction with nuclei of protons, neutrons, pions and kaons in the approximate energy range 20 GeV–50 TeV. When coupled to gamma-nuclear models, QGS is also valid for incident high energy photons. Additional models are required to fragment and de-excite the damaged nucleus which remains after the initial high energy interaction. The model handles the selection of collision partners, splitting of the nucleons into quarks and di-quarks, the formation and excitation of quark–gluon strings, string hadronization and diffractive dissociation.

The modeling sequence begins by building a 3-D model of the target nucleus. Nucleon momenta are sampled using the Fermi gas model. The nuclear density is assumed to have a Woods–Saxon shape for all nuclei with $A \geq 17$. For lighter nuclei a harmonic oscillator shape is used. The momentum sampling is done in a correlated manner, with local phase space densities constrained by the Pauli principle and the sum of all nucleon momenta constrained to zero. The Baker and Ter-Martirosyan (1976) approach is used to determine the probability of an inelastic collision with each nucleon. The initial interaction is assumed to proceed by pomeron exchange between the interacting hadrons. String formation follows the method of Capella and Krzywicki (1978) and Kaidalov and Ter-Martirosyan (1982) in which the parton densities are sampled for each participating hadron. The transverse momentum of each hadron is sampled from a Gaussian distribution with $\langle P_t^2 \rangle = 0.5\,\mathrm{GeV}^2$ while the longitudinal momentum is sampled from fragmentation functions native to the Geant4 QGS code. The amount of diffractive dissociation is chosen empirically.

The simulation predictions of the QGS model are in good agreement with experimental data at high energies (Figs. 8 and 9).

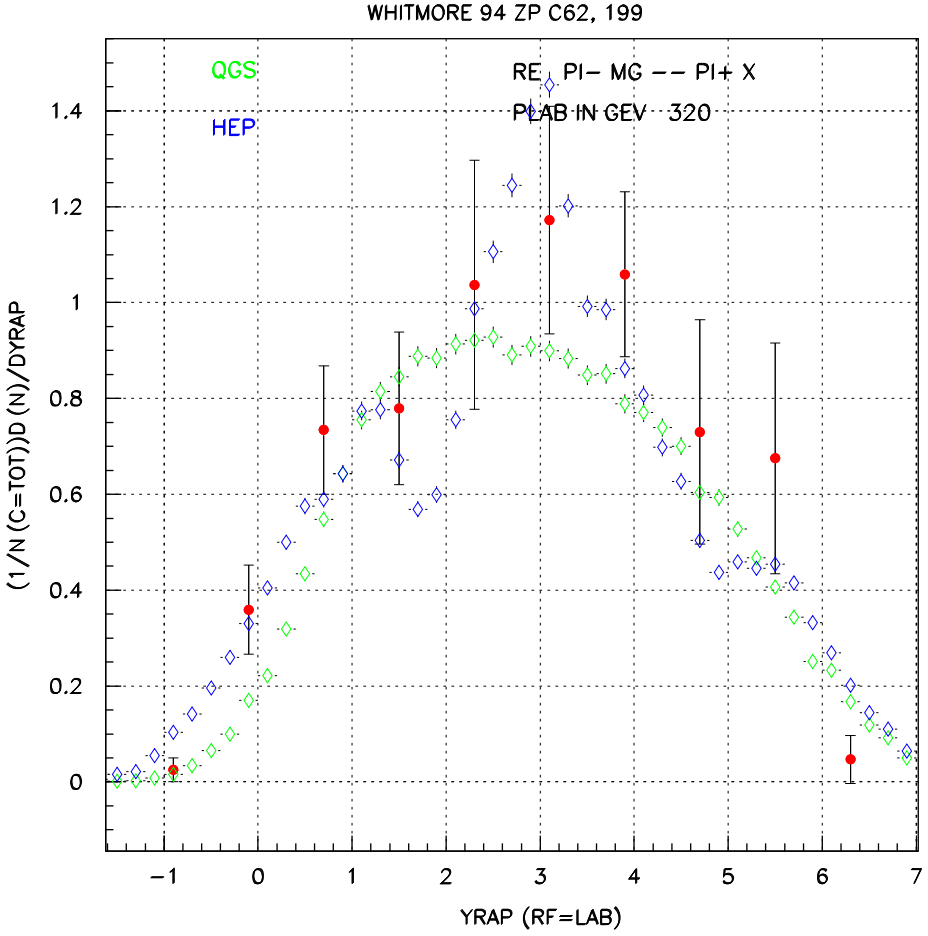

Fig. 8. Secondary π^+ production by 320 GeV π^- in magnesium. The π^+ rapidity distribution: close circles data (Whitmore et al., 1994); open circles—QGS model predictions (Geant4 8.1).

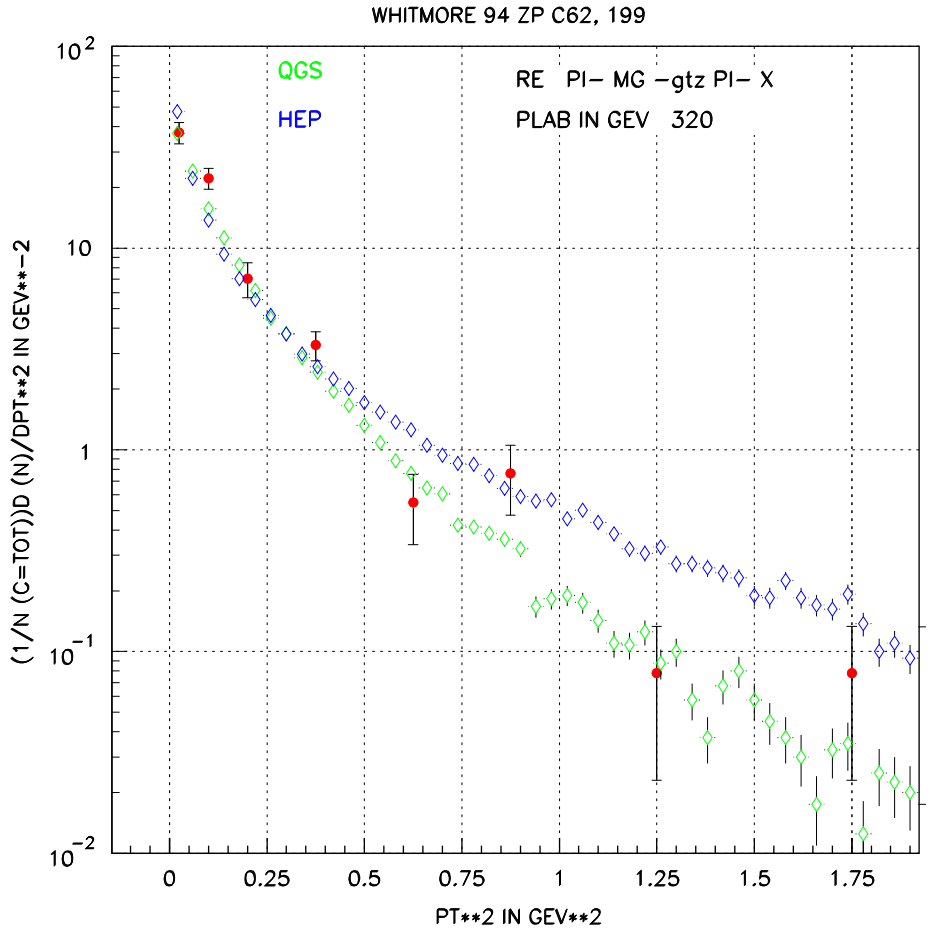

Fig. 9. Secondary π^- production by 320 GeV π^- in magnesium. The π^- transverse momentum square distribution: close circles data (Whitmore et al., 1994); open circles—QGS model predictions (Geant4 8.1).

It is used by the main LHC detectors (Stavrianakou, 2004; Rimoldi, 2004; Mato et al., 2004) as the main simulation production engine.

4.3. *Bertini-style cascade*

In the cascade energy range Geant4 has a Bertini-style cascade model (Heikkinen et al., 2003) which handles incident protons, neutrons, pions, kaons and hyperons up to 10 GeV. The implementation employs many of the standard intra-nuclear cascade features developed by Bertini and Guthrie (1971). Three of these are:

- classical scattering without matrix elements;
- free hadron–nucleon cross sections and angular distributions which are taken from experiment; and
- step-like nuclear density distributions and potentials.

The second feature, in principle, allows the model to be extended to any particle for which there are sufficient double-differential cross section measurements.

The projectile enters the nucleus at a point sampled over the projected area of the nucleus. The projectile is then transported along straight lines through the nuclear medium and interacts according to the mean free path determined by the free hadron-nucleon total cross section. The nuclear medium is approximated by up to three concentric, constant-density shells. The initial nucleon momenta are distributed according to the Fermi gas model, and Pauli blocking is invoked for the nucleons. For the most part the projectile interacts with a single nucleon, but some nucleon–nucleon correlation is included by allowing pions to be absorbed on quasi-deuterons.

Each secondary from initial and subsequent interactions is also propagated in the nuclear potential until it interacts or leaves the nucleus. During propagation, particles may be reflected from, as well as transmitted through, the shell boundaries mentioned above. One drawback of the current model is that there is no Coulomb barrier implemented, thus the low energy proton spectrum is incorrectly modeled.

As cascade collisions occur, an excited residual nucleus is built up. This is done by forming particle–hole states based on the selection rules:

$$\Delta p = 0, \pm 1, \quad \Delta h = 0, \pm 1, \quad \Delta n = 0, \pm 2. \tag{6}$$

The Bertini-style cascade has its own exciton routine which is used to collapse the particle–hole states and de-excite the residual nucleus using the approach (Griffin, 1966). The transition from cascade stage to exciton stage occurs when the secondary kinetic energy drops below either 20% of its original value, or seven times the nuclear binding energy. For light, highly excited nuclei Fermi breakup may occur, and fission is also possible. In the final stage, nuclear evaporation occurs as long as the excitation energy is large enough to remove a neutron or alpha from the nucleus. Gamma emission then occurs at energies below 0.1 MeV.

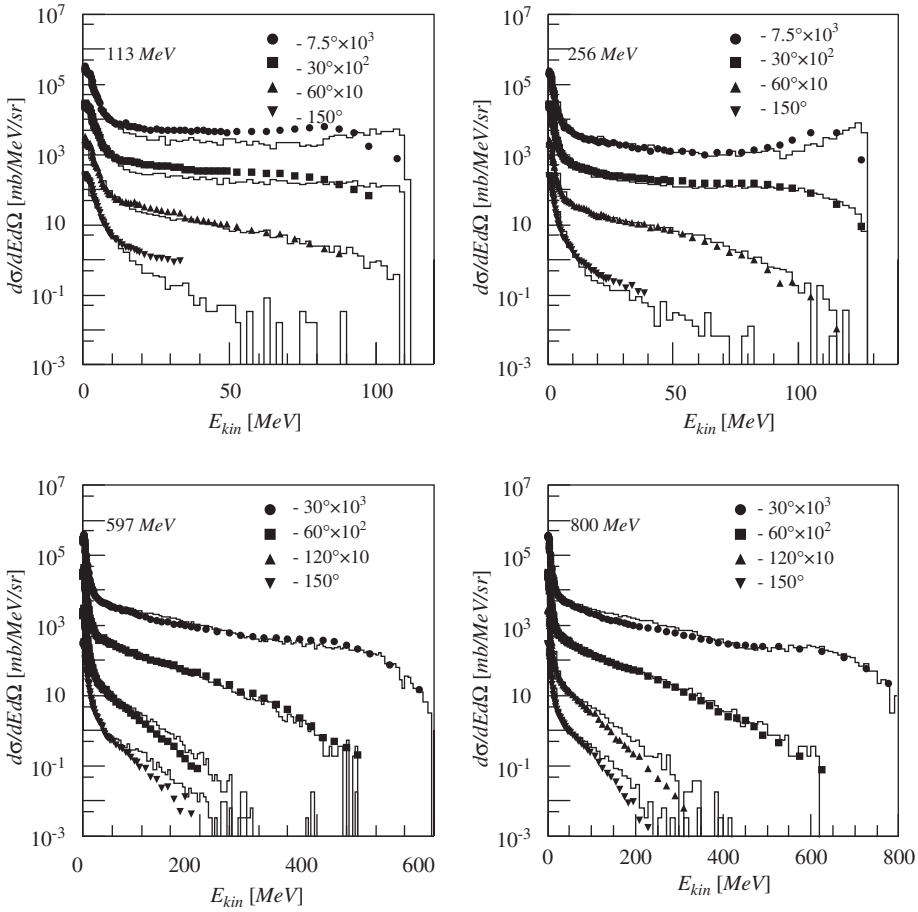

Fig. 10. Double differential cross section for neutrons produced in proton scattering off lead. Points: data (Meier et al., 1989, 1992; Amian et al., 1992, 1993); histograms: Betrini-style cascade predictions (Geant4 8.1).

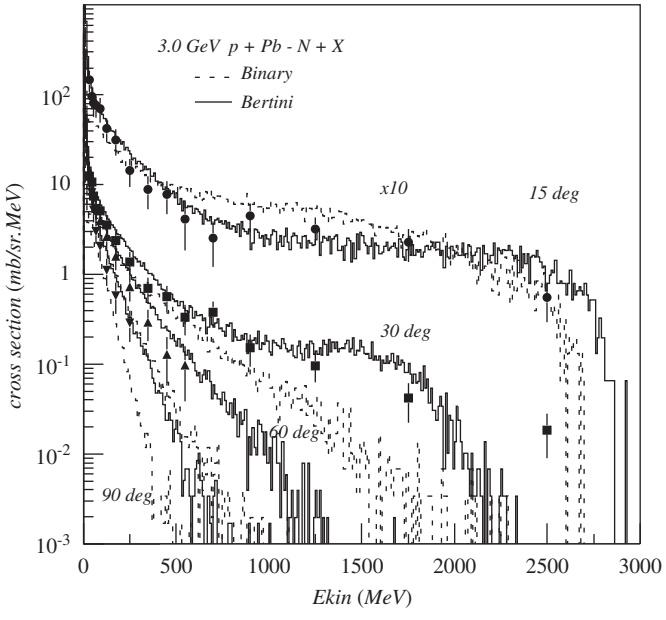

Fig. 11. Double differential cross section for neutrons produced in proton scattering off lead at 3 GeV. Points: data (Ishibashi et al., 1997); histograms: Geant4 8.1 predictions, solid—the Betrini-style cascade, dotted—the Binary cascade.

The validation of Geant4 cascades is performed using thin target data. The simulation predictions of the Bertini-style cascade for double differential cross sections of secondary neutron production by protons in lead versus experimental data are shown in Fig. 10. The agreement is reasonable at low energies (100–200 MeV) and is very good at 800 MeV. The comparison with the relatively new data at 3 GeV (Fig. 11) shows that predictions of the Bertini-style cascade are good both at forward and backward angles. The isotope production cross sections (Fig. 12) is also in a good agreement with the data.

4.4. Binary cascade

A more theoretically motivated alternative to the Bertini-style cascade is the Geant4 Binary cascade model (Folger et al., 2004), which is a hybrid between a classical cascade and a full quantum-molecular dynamics model. It was designed for incident protons and neutrons with $0<E_{kin}<3$ GeV, pions with $0<E_{kin}<1.5$ GeV, and light ions with $0<E_{kin}<3$ GeV/A. However, it works reasonably well up to 10 GeV when compared to the Bertini-style cascade.

A detailed 3-D model of the nucleus is used, placing nucleons in space according to Woods–Saxon-shaped nuclear densities, and in momentum according to the Fermi gas model. The nucleon momentum is taken into account when evaluating cross sections and collision probabilities. An optical potential is included to simulate the collective effect of the nucleus on the nucleons participating in the reaction. The incident particle and subsequent secondaries are then propagated through the nucleus along curved paths by numerical integration of the equation of motion in the potential.

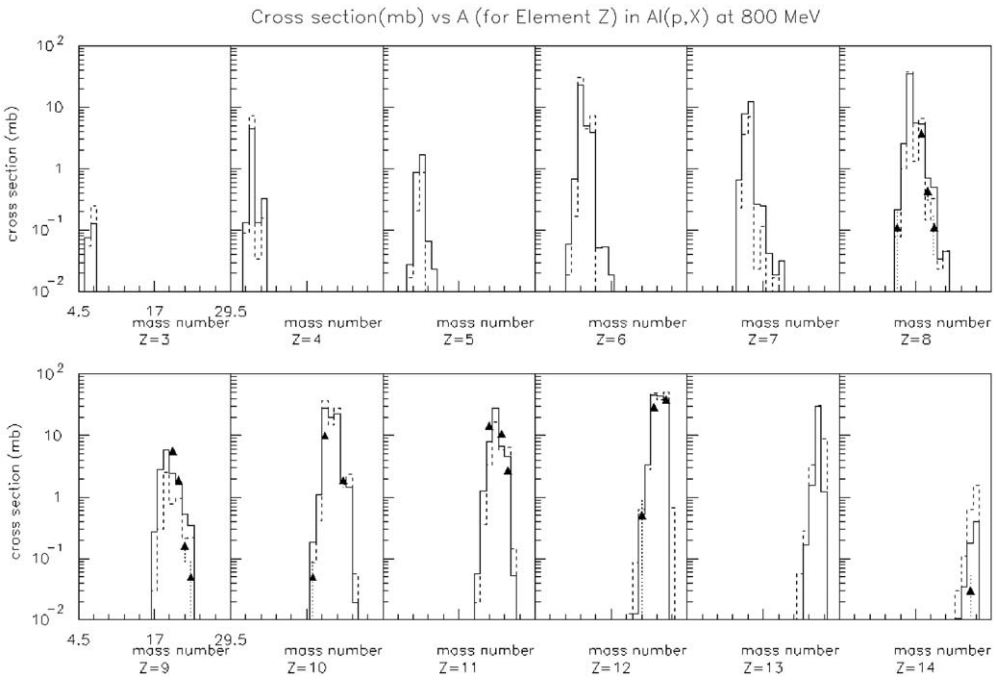

Fig. 12. Probability of different isotope production by proton collision off ^{12}C. Points: data (Vonach et al., 1997); solid histogram: Bertini-style cascade predictions; dashed histograms: Binary cascade predictions (Geant4 8.1).

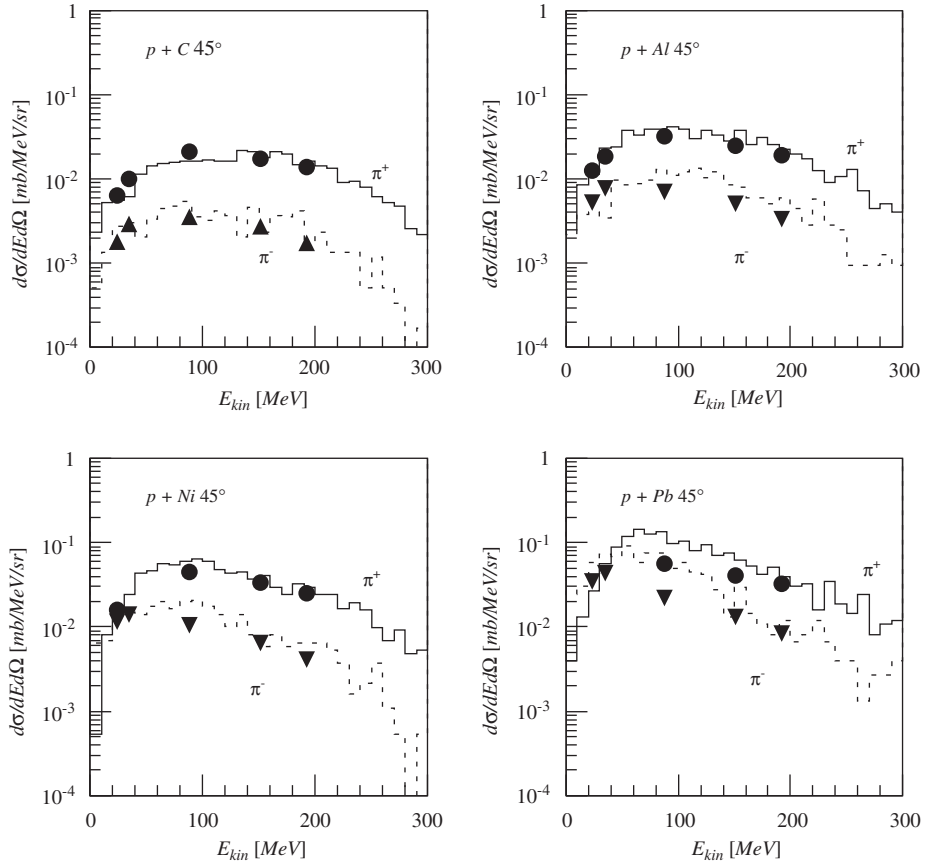

Fig. 13. Double differential cross section for charged pions produced in 585 MeV proton scattering off different materials. Points: data (Crawford et al., 1980); histograms: Binary cascade predictions (Geant4 8.1).

Nucleon–nucleon scattering is handled by t-channel resonance formation and decay. The excitation cross sections are derived from $p-p$ scattering using isospin invariance and the corresponding Clebsch–Gordan coefficients. Elastic nucleon–nucleon scattering is also included. Meson–nucleon inelastic scattering, except for true absorption, is modeled as s-channel resonance excitation. Here, the Breit–Wigner form is used for the cross sections.

Once resonances are formed, they may interact or decay. At present the Binary cascade model takes into account 25 strong resonances: 10 delta resonances from 1232 to 1950 MeV, and 15 nucleon resonances from 1440 to 2250 MeV. It is the mass of the highest included resonances which currently limits the upper energy of the model's validity. Nominal PDG branching ratios are used for resonance decay and the masses are sampled from the Breit–Wigner shape. The imaginary part of the R-matrix is calculated using free two-body cross sections from experimental data and parameterizations.

Cascade models are generally not valid for energies below a few tens of MeV. For the binary model, the cascade stops when the mean energy of all scattered particles is below an A-dependent cut, which varies from 18 to 90 MeV. Below this energy, the properties of the residual nucleus and exciton system, which are built up during the cascade, are passed to the Geant4 precompound model (Geant4 Collaboration, 2003) which handles the nuclear de-excitation. When the primary particle is below 45 MeV, the cascade is not initiated; instead control is passed directly to the precompound model.

The predictions of the Binary cascade for the differential cross sections of secondary neutron production for proton beam with energy below 1 GeV is very good (Folger et al., 2004) and it is a key advantage of the Binary cascade in comparison with the Bertini-style cascade. Recent improvements provide more precise results for the inclusive production of change pions (Fig. 13). The prediction for the isotope production cross sections is very reasonable (Fig. 12) and the results of the Binary cascade for ion-ion interactions at relatively low energies are also very promising (Fig. 14). However, the Binary cascade cannot replace the Bertini-style cascade, because for high incident proton energies (Fig. 11) the Binary cascade currently overestimate forward neutron cross section and underestimate backward neutron cross section. Also Binary cascade simulation is slower, especially for heavy targets, so user needs to configure Geant4 hadronic physics according to requirements for a simulation application.

4.5. Chiral invariant phase space model

The CHIPS model began as an event generator and was incorporated into Geant4 as a novel way of treating the anti-baryon-nucleon annihilation (Degtyarenko et al., 2000), capture of negatively charged hadrons at rest (Degtyarenko et al., 2001a), gamma- and lepto-nuclear reactions (Degtyarenko et al., 2001b). It is also used in some Geant4 models to handle the nuclear fragmentation part of nuclear de-excitation. CHIPS is based on a few main concepts:

- the quasmon—an ensemble of massless partons uniformly distributed in invariant phase space. This is a 3-D bubble of quark–parton plasma and can be any excited hadron system or ground state hadron;

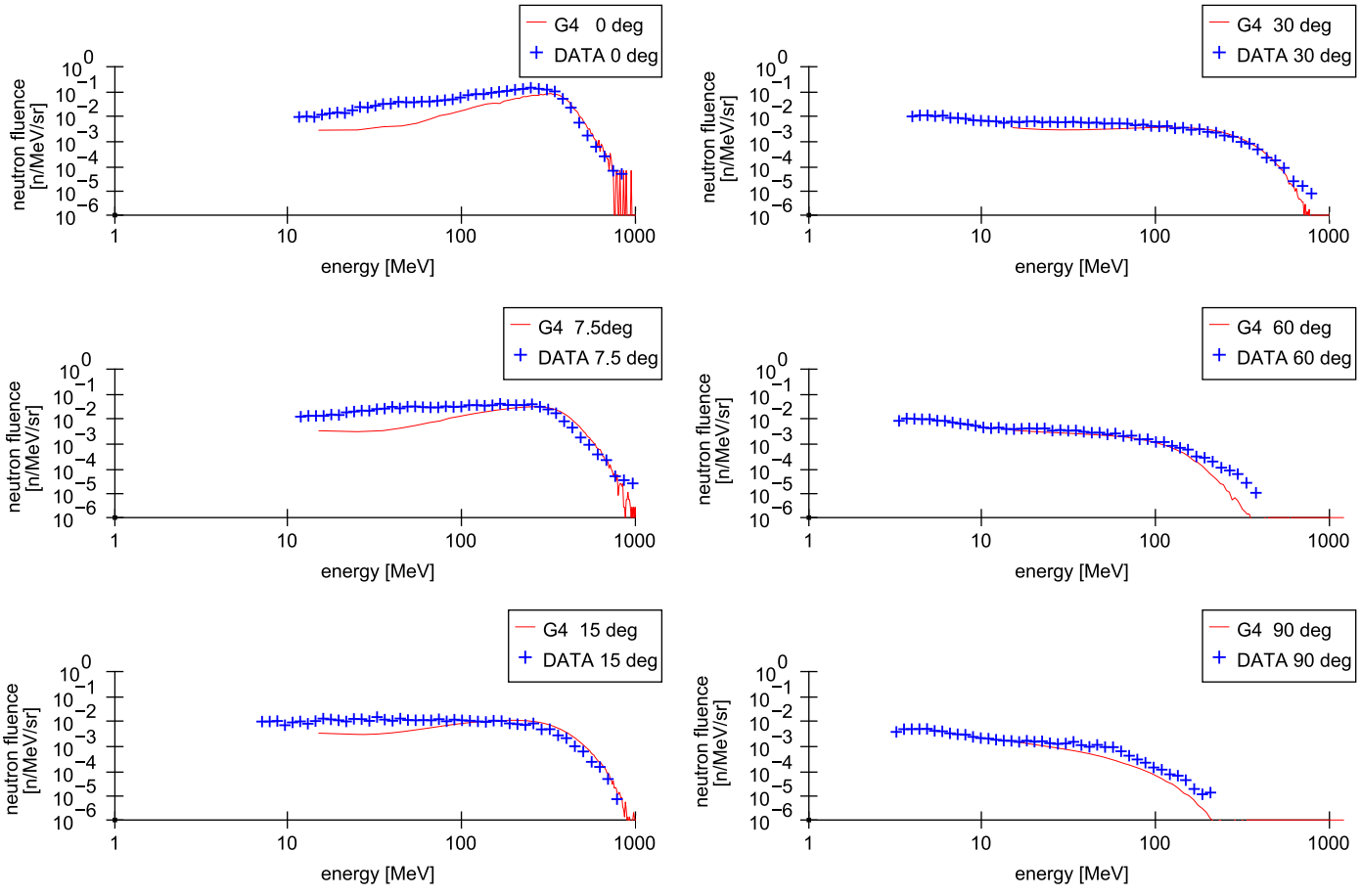

Fig. 14. Double differential cross section for neutrons produced in ^{56}Fe scattering off aluminum. Points: data (Kurosawa et al., 2000); histograms: Binary cascade predictions (Geant4 8.1).

- critical temperature T_c—a model parameter which relates the quasmon mass M_Q to the number of its partons n:

$$M_Q^2 = 4n(n-1)T_c^2 \rightarrow M_Q \simeq 2nT_c, \quad (7)$$

$$T_c = 180-200\text{MeV}; \quad (8)$$

- quark fusion hadronization—two quark–partons may combine to form a hadron and
- quark exchange hadronization—quarks from quasmon and neighboring nucleon may trade places.

The model treats u, d and s quarks symmetrically assuming them to be massless. It can produce kaons, but to get kaon multiplicities correct, a strangeness suppression parameter is required and in addition an η suppression parameter is used. The real s-quark mass is taken into account in masses of produced strange hadrons.

As the maximum energy from the primary quark parton contributes to the inclusive spectra the quark exchange or fission can be considered as a 1-D process. It is demonstrated experimentally by the fact that when the inclusive hadron spectra are plotted versus $k = (p + E_{kin})/2$, they not only have the same exponential slope but nearly coincide.

The modeling sequence for CHIPS simulation varies somewhat according to the application. The initial state generation is different for the case of proton–anti-proton annihilation (Degtyarenko et al., 2000), negatively charged pion capture (Degtyarenko et al., 2001a), photo-nuclear and lepto-nuclear (Degtyarenko et al., 2001b) processes. All these processes are included by default in the main physics configurations provided with the Geant4 release 8.1 and later. The quality of the CHIPS model predictions can be demonstrated for the π^- capture at rest (Fig. 15). This process is very frequent in hadronic showers and secondary spectra of protons, neutrons, and light nuclei are important for simulation of the responses in HEP experiments.

4.6. Physics configuration

The Geant4 toolkit offers a variety of options for physics processes and models over a wide range of energies of electromagnetic and strong interactions. They are configured for the particular application via the *Physics Lists* interface. The level of accuracy and speed of the models are different and a unique effective theory for hadronic interactions is absent. These circumstances justify the necessity of applying alternative physics models for the different use-cases. The Geant4 physics configuration was initially assumed to be the responsibility of the user (Geant4 Collaboration, 2003). However, simulation practice requires a provision of reference configurations of Geant4 physics models, so reference Physics Lists were created and delivered together with the source code of recent Geant4 releases (Allison et al., 2006).

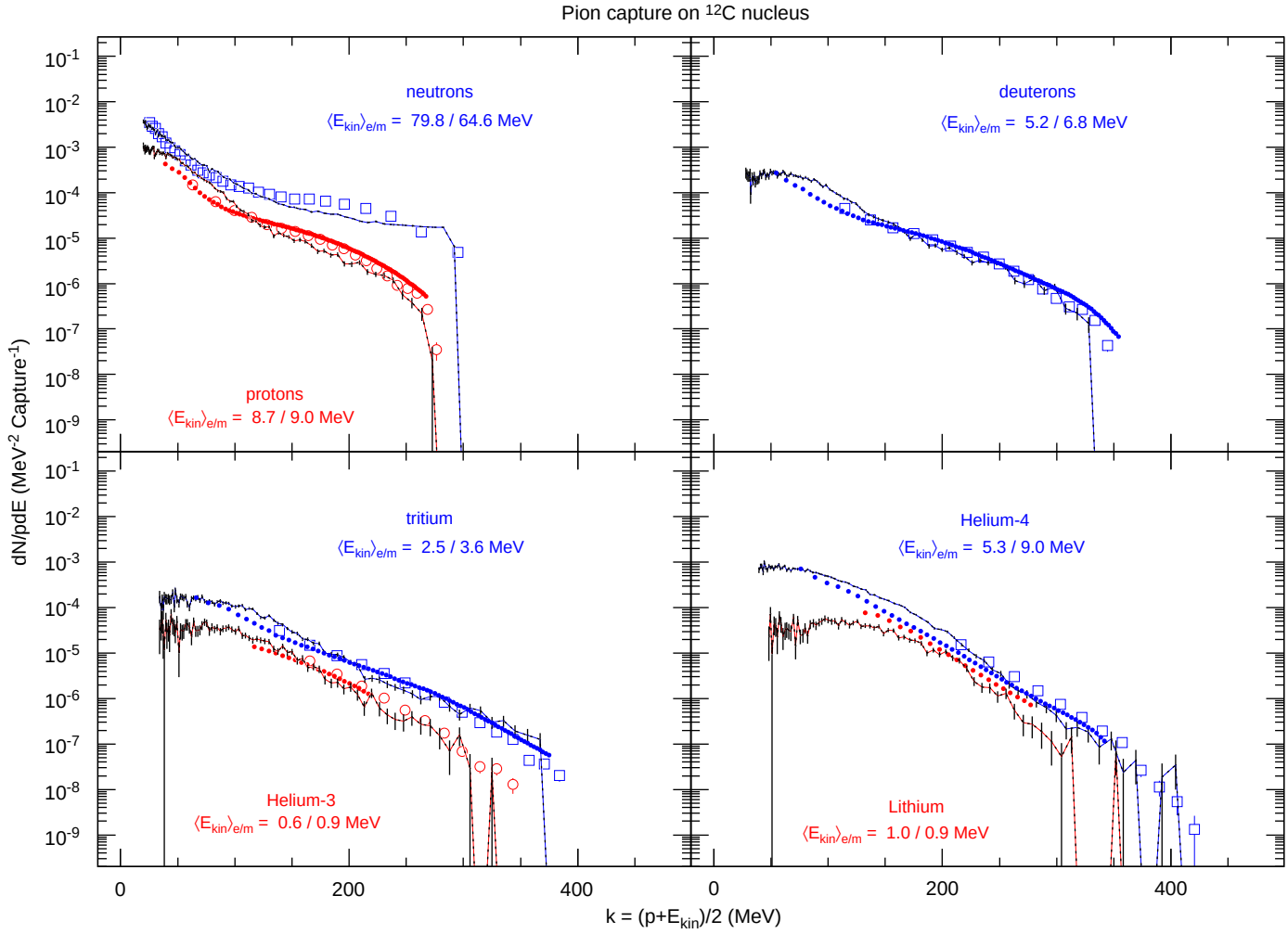

Fig. 15. The differential cross sections of secondary particle production in π^- capture off carbon as a function of the kinematical parameter $k = (p + E_{kin})/2$. Points: data (see references in Degtyarenko et al., 2001a); histograms: CHIPS model predictions (Geant4 8.1).

The Physics List QGSP_BERT is proposed currently for typical HEP applications. It includes the Standard EM component, the QGS model for high energy hadron inelastic interactions, the Bertini-style cascade for the hadron inelastic interactions below 10 GeV and other physics components: ion inelastic interactions; hadron elastic scattering; negative particles capture at rest; gamma- and electro-nuclear interaction.

For applications with initial energies of particles below 1 GeV the Binary cascade for hadrons and ions is proposed as more advanced. This configuration is provided with the QGSP_BIC Physics List, which is relevant to a variety of radiation studies.

A number of other reference Physics Lists are supported and also some additional Physics Lists are included in Geant4 examples. The user software built on top of Geant4 can have its own configuration of the Geant4 physics. For example, the GATE software (Jan et al., 2004) created for medical applications is providing configurations of both Standard and Low-energy EM packages. The GRAS software (Santin et al., 2005), created for studies of space radiation effects, is also providing different alternative configurations in addition to the standard Geant4 physics: PAI model of ionization, Low-energy EM physics, high precision neutron transport, radioactive decays.

5. Conclusions

The Geant4 toolkit is used in Monte Carlo production for HEP applications and for different applications for radiation detectors, for space and medicine. The recent upgrades of the toolkit increase its capabilities. In this work we emphasize the progress made for the geometry modeler of Geant4, the upgrade in the materials, and in the standard electromagnetic and hadronic physics. The validation results demonstrate that the upgrade of the multiple scattering model improves significantly the simulation precision for sampling calorimeters and, in general, for simulation of electron transport across a boundary between different media. The results of validation of hadronic generators discussed above show that the standard set of hadronic models reproduces well the main processes of hadronic interaction with matter.

References

Allison, J., et al., 2006. Geant4 developments and applications. IEEE Trans. Nucl. Sci. 53 (1), 270–278.

Allisy, A., et al., 1993. Stopping powers and ranges for protons and alpha particles. ICRU Report 49.

Amako, K., et al., 2005. Comparison of Geant4 electromagnetic physics models against NIST reference data. IEEE Trans. Nucl. Sci. 52 (4), 218–910.

Amian, W.B., et al., 1992. Differential neutron production cross sections for 800-MeV protons. Nucl. Sci. Eng. 112 (1), 78–86.

Amian, W.B., et al., 1993. Differential neutron production cross sections for 597-MeV protons. Nucl. Sci. Eng. 115 (1), 1–12.

Anninos, D., et al., 2006, Recent developments and upgrades to the Geant4 geometry modeller. In: Proceedings of the CHEP'06 Conference, Mumbai, India, February.

Apostolakis, J., et al., 1999. Geant4 low energy electromagnetic models for electrons and photons. CERN-OPEN-99-034, Geneva; INFN/AE-99/18, Frascati.

Apostolakis, J., et al., 2000. The implementation of ionization energy loss in very thin absorbers for the Geant4 simulation package. Nucl. Instrum. Meth. A 453 (3), 597.

Apostolakis, J., et al., 2006. The recent upgrades in the Standard electromagnetic physics package. In: Proceedings of the CHEP'06 Conference, Mumbai, India, February.

Archambault, J.P., Gumplinger, P., et al., 2003. GEANT4 photon readout simulations of plastic scintillating strips with embedded WLS fibers. In: Nuclear Science Symposium Conference Record 2003 IEEE, vol. 3, pp. 1549–1551.

BABAR Collaboration (Aubert, B., et al.), 2002. The BABAR detector. Nucl. Instrum. Meth. A 479 (1), 1–116.

Baker, M., Ter-Martirosyan, K.A., 1976. Gribov's Reggeon calculus: its physics basis and implications. Phys. Rep. 28 (1), 1–143.

Bertini, H.W., Guthrie, M.P., 1971. New item results from medium-energy intranuclear-cascade calculation. Nucl. Phys. A 169 (3), 670–672.

Bogdanov, A.G., et al., 2006. Geant4 simulation of production and interaction of muons. IEEE Trans. Nucl. Sci. 53 (2), 513–519.

Booth, T., 1985. A sample problem for variance reduction in MCNP. Los Alamos National Laboratory Report LA-10363-MS, October.

Burkhardt, H., et al., 2005. GEANT4 standard electromagnetic physics package. In: Proceedings of MC2005, Chattanooga, TN. American Nuclear Society, LaGrange Park, IL, April 17–21 (on CD-ROM).

Burkhardt, H., 2007. Monte Carlo generation of the energy spectrum of synchrotron radiation. CLIC - Note - 709, EUROTEV - Report - 2007 - 012.

Capella, A., Krzywicki, A., 1978. Unitary corrections to short range order: long range rapidity correlations. Phys. Rev. D 18 (11), 4120–4133.

Chauvie, S., et al., 2004. Geant4 low energy electromagnetic physics. In: Conference Record 2004 IEEE Nuclear Science Symposium, vol. 3, pp. 1881–1885.

Chauvie, S., et al., 2006. Monte Carlo simulation of interactions of radiation with biological systems at the cellular and DNA levels: the Geant4-DNA project. Radiat. Res. 166, 676–677.

Chytracek, R., McCormick, J., Pokorski, W., Santin, G., 2006. Geometry description markup language for physics simulation and analysis applications. IEEE Trans. Nucl. Sci. 53 (5), 2892–2896.

Cirrone, G.A.P., et al., 2005. Implementation of a new Monte Carlo—GEANT4 simulation tool for the development of a proton therapy beam line and verification of the related dose distributions. IEEE Trans. Nucl. Sci. 52 (1), 262–265.

Coursey, J.S., Schwab, D.J., Dragoset, R.A., 2005. Atomic Weights and Isotopic Compositions, version 2.4.1. National Institute of Standards and Technology, Gaithersburg, MD. Available http://physics.nist.gov/PhysRefData/. Originally published as Coplen, T.B., 2001. Atomic weights of the elements 1999. Pure Appl. Chem. 73 (4), 667; Rosman, K.J.R., Taylor, P.D.P., 1998. Isotopic compositions of the elements 1997. J. Phys. Chem. Ref. Data 27 (6), 1275; Audi, G., Wapstra, A.H., 1995. The 1995 update to the atomic mass evaluation. Nucl. Phys. A 595 (4), 409.

Crawford, J.F., et al., 1980. Measurement of cross sections and asymmetry parameters for production of charged pions from various nuclei by 585-MeV protons. Phys. Rev. C 22 (3), 1184–1196.

Degtyarenko, P.V., Kossov, M.V., Wellisch, H.P., 2000. Chiral invariant phase space event generator. I. Nucleon–antinucleon annihilation at rest. Eur. Phys. J. A 8 (2), 217–222.

Degtyarenko, P.V., Kossov, M.V., Wellisch, H.P., 2001a. Chiral invariant phase space event generator. II. Nuclear pion capture at rest and photonuclear reactions below the $\Delta(3,3)$ resonance. Eur. Phys. J. A 9 (2), 211–220.

Degtyarenko, P.V., Kossov, M.V., Wellisch, H.P., 2001b. Chiral invariant phase space event generator. II. Model of real and virtual photon interactions with nuclei below pion production threshold. Eur. Phys. J. A 9 (2), 221–224.

Dressel, M., 2003. Geometrical importance sampling in Geant4: from design to verification. CERN-OPEN-2003-048.

Fesefeld, H., 1985. Simulation of hadronic showers, physics and applications. Technical Report PITHA 85-02, Aachen, Germany, September 1985.

Folger, G., Wellisch, H.P., 2003. String parton models in Geant4. In: Proceedings of CHEP03 Conference, La Jolla, CA, March 2003, nucl-th/0306007.

Folger, G., Ivanchenko, V.N., Wellisch, J.P., 2004. The binary cascade. Eur. Phys. J. A 21 (3), 407–417.

Giani, S., et al., 1999a. Geant4 simulation of energy losses of slow hadrons. CERN-OPEN-99-121, Geneva; INFN/AE-99/20, Frascati.

Giani, S., et al., 1999b. Geant4 simulation of energy losses of ions. CERN-OPEN-99-300, Geneva; INFN/AE-99/21, Frascati.

Geant4 Collaboration (Agostinelli, S., et al.), 2003. Geant4—a simulation toolkit. Nucl. Instr. Meth. A 506(3), 250–303.

Grichine, V.M., 2002. Generation of X-rays transition radiation inside complex radiators. Phys. Lett. B 525 (3–4), 225–239.

Griffin, J.J., 1966. Statistical model of intermediate structure. Phys. Rev. Lett. 17 (9), 478–481.

Heikkinen, A., Stepanov, N., Wellisch, H.P., 2003. Bertini intra-nuclear cascade implementation in Geant4. In: Proceedings of CHEP03 Conference, La Jolla, CA, March, nucl-th/0306008.

Ivanchenko, V.N., Bukin, A.D., et al., 1991, UNIMOD2: universal Monte Carlo for simulation of e^+e^- experiments. In: Proceedings of MC1991, Detector and Event Simulation in High Energy Physics, Amsterdam, pp. 79–85. HEP INDEX 30, 1992, No. 3227.

Ivanchenko, V.N., 2002. Geant4: physics potential for HEP instrumentation. Nucl. Instrum. Meth. A 494 (1–3), 514–519.

Ivanchenko, V.N. (on behalf of Geant4 Collaboration), 2004. Geant4: physics potential for instrumentation in space and medicine. Nucl. Instrum. Meth. A 525 (1–2), 402–405.

Ishibashi, K., et al., 1997. Measurement of neutron-production double-differential cross sections for nuclear spallation reaction induced by 0.8, 1.5 and 3.0 GeV protons. J. Nucl. Sci. Technol. 34 (6), 529–537.

Jan, S., et al., 2004. GATE: a simulation toolkit for PET and SPECT. Phys. Med. Biol. 49, 4543–4561.

Kawrakow, I., Bielajew, A.F., 1998. On the condensed history technique for electron transport. Nucl. Instrum. Meth. B 142 (1), 253–280.

Kurosawa, T., et al., 2000. Neutron yields from thick C, Al, Cu, and Pb targets bombarded by 400 MeV/nucleon Ar, Fe, Xe 800 MeV/nucleon and 800 MeV/nucleon Si ions. Phys. Rev. C 62 (4), 044615–044624.

Kaidalov, A.B., Ter-Martirosyan, K.A., 1982. Pomeron as quark–gluon string and multiple hadron production at SPS-collider energies. Phys. Lett. B 117 (3–4), 247–251.

Lassila-Perini, K., Urban, L., 1995. Energy loss in thin layers in GEANT. Nucl. Instrum. Meth. A 362 (2–3), 416–422.
Lewis, H.W., 1950. Multiple scattering in an infinite medium. Phys. Rev. 78 (5), 526–529.
Mato, P., Charpentier, P., Corti, G., et al., 2004. Software for the LHCb experiment. In: IEEE NSS-38-10 Conference Record.
Meier, M.M., et al., 1989. Differential neutron production cross sections and neutron yields from stopping-length targets for 113-MeV protons. Nucl. Sci. Eng. 102 (1), 310–321.
Meier, M.M., et al., 1992. Differential neutron production cross sections for 256-MeV protons. Nucl. Sci. Eng. 110 (1), 289–298.
Pia, M.G. (on behalf of Geant4 Collaboration), 2003. The Geant4 toolkit: simulation capabilities and application results. Nucl. Phys. B Proc. Suppl. 125, 60–68.
Poon, E., Verhaegen, F., 2005. Accuracy of the photon and electron physics in GEANT4. Med. Phys. 32 (6), 1696–1711.
Rimoldi, A. (on behalf of the ATLAS Simulation Group), 2004. The simulation for the ATLAS experiment: present status and outlook. In: IEEE NSS-33-166 Conference Record.
Santin, G., Ivanchenko, V., et al., 2005. GRAS: a general-purpose 3-D modular simulation tool for space environment effect analysis. IEEE Trans. Nucl. Sci. 52 (6), 2294–2299.
Smith, D.A. (on behalf of the BaBar Computing Group), 2004. A millennium of work in under a year BaBar simulation program. In: IEEE NSS-38-1 Conference Record.
Stavrianakou, M. (on behalf of the CMS Collaboration), 2004. An object-oriented simulation program for CMS. In: IEEE NSS-38-3 Conference Record.
Urban, L., 2002, Multiple scattering model in Geant4. CERN-OPEN-2002-070.
Urban, L., 2006. A model of multiple scattering in Geant4. CERN-OPEN-2006-077.
Vonach, H., et al., 1997. Spallation reactions in ^{27}Al and ^{56}Fe induced by 800 MeV protons. Phys. Rev. C 55 (5), 2458–2467.
Whitmore, J.J., et al., 1994. Inclusive charged pion production in hadron-nucleus interactions at 100 and 320 GeV/c. Z. Phys. C 62 (2), 199–227.